Available online at www.sciencedirect.com

ScienceDirect

Nuclear Physics B 926 (2018) 49–69

NUCLEAR PHYSICS B

www.elsevier.com/locate/nuclphysb

Black hole remnants in Hayward solutions and noncommutative effects

S. Hamid Mehdipour *, M.H. Ahmadi

Department of Physics, College of Basic Sciences, Lahijan Branch, Islamic Azad University, P.O. Box 1616, Lahijan, Iran

Received 28 April 2016; received in revised form 2 June 2017; accepted 26 September 2017
Available online 29 September 2017
Editor: Leonardo Rastelli

Abstract

In this paper, we explore the final stages of the black hole evaporation for Hayward solutions. Our results show that the behavior of Hawking's radiation changes considerably at the small radii regime such that the black hole does not evaporate completely and a stable remnant is left. We show that stability conditions hold for the Hayward solutions found in the Einstein gravity coupled with nonlinear electrodynamics. We analyze the effect that an inspired model of the noncommutativity of spacetime can have on the thermodynamics of Hayward spacetimes. This has been done by applying the noncommutative effects to the non-rotating and rotating Hayward black holes. In this setup, all point structures get replaced by smeared distributions owing to this inspired approach. The noncommutative effects result in a colder black hole in the small radii regime as Hayward's free parameter g increases. As well as the effects of noncommutativity and the rotation factor, the configuration of the remnant can be substantially affected by the parameter g. However, in the rotating solution it is not so sensitive to g with respect to the non-rotating case. As a consequence, Hayward's parameter, the noncommutativity and the rotation may raise the minimum value of energy for the possible formation of black holes in TeV-scale collisions. This observation can be used as a potential explanation for the absence of black holes in the current energy scales produced at particle colliders. However, it is also found that if extra dimensions do exist, then the possibility of the black hole production at energy scales accessible at the LHC for large numbers of extra dimensions will be larger.

* Corresponding author.
E-mail addresses: mehdipour@liau.ac.ir (S.H. Mehdipour), ahmadi@liau.ac.ir (M.H. Ahmadi).

https://doi.org/10.1016/j.nuclphysb.2017.09.021

1. Introduction

Black holes (BHs) and singularities are accepted to be unavoidable predictions of the theory of general relativity [1]. It is widely believed that only a not yet attainable quantum gravity theory would be capable to study the issue of central singularity of a BH properly. However, various phenomenological approaches have been considered in the literature in order to solve the problem of BH's singularity with a regular center [2]. The Bardeen BH [3] is the first regular model which has proposed as a spherically symmetric compact object with an event horizon and without violating the weak energy condition. The inside of its horizon is de Sitter-like wherein the matter has a high pressure. In 2006, the formation and evaporation of a new kind of regular solutions was studied by Hayward [4]. The static region of a Hayward spacetime is Bardeen-like while the dynamic regions are Vaidya-like. A general class of regular solutions utilizing a mass function that generalizes the Bardeen and Hayward mass terms have been suggested [5]. The authors of Ref. [6] have discussed the massive scalar quasinormal modes of the Hayward BH (H-BH). The motion of a particle in background of a H-BH has been studied [7]. The accretion of fluid flow around the modified H-BH has been investigated [8]. Recently, the effects of thermal fluctuations on thermodynamics of a modified H-BH have also been analyzed [9]. There have been a great number of studies concerning regular BHs in the recent literature [10–14].

It was shown that the physical source of Regular BHs can be interpreted as the gravitational field of a nonlinear electrodynamics (NED) [15–18]. The NED was founded by Born and Infeld [19]. The NED theories emerge from low-energy effective limits in specific models of string/M-theories [20–22]. There are two basic aims in a NED theory. The first is to consider electromagnetic field and particles within the context of a physical source. The other great aim is to avoid letting physical quantities become infinite. A similar procedure can be achieved by the NED coupled to gravity in such a way that regular spherically symmetric electrically charged solutions confirm the weak energy condition and have an unavoidable de Sitter center. The Regular BH solutions to Einstein equations with physically reasonable sources have been introduced by Ayon-Beato and Garcia [15–17]. In this model, the Bardeen BH was reinterpreted as a magnetic solution to Einstein equations with NED [18]. The regular BH solution in the $f(T)$ gravity coupled to NED has been found in [23]. The other solutions of the combined Einstein and NED equations have also been reported [24–26]. For considerably more details concerning the nonlinear effects we suggest the following literature [27–34].

In addition, on the other hand, it is well-known that the appearance of high energies in a noncommutative manifold is a consequence of quantum fluctuation effects at very short distances wherein any measurements to determine a particle position with an accuracy more than an innate minimal length scale, namely the Planck length, are hindered. Noncommutative BHs are naturally identified with the possible running of this minimal length scale in BH physics. Based on an inspired noncommutative model [35–39], instead of describing a point particle as a Dirac-delta function distribution, it is characterized by a Gaussian function distribution with a minimal width $\sqrt{\theta}$, i.e. a smeared particle, where θ is the smallest fundamental cell of an observable area in the noncommutative spacetime, beyond which coordinate resolution is not obvious. In this model, the energy-momentum tensor takes a new form, while the Einstein tensor remains unchanged. As an important result, the curvature singularity at the center of noncommutative BHs is eliminated. This means that Planck scale physics may prevent the appearance of a singularity in the center of a BH wherein a BH remnant may be formed (for an extensive review of BH remnants, see [40]).

In the group of various BH solutions, the rotating ones, without any hesitations, are most suitable to fit the observational data proving that collapsed objects display high angular momenta.

The BH spin plays a fundamental role in any astrophysical process. Hence, its perfect comprehension is essential for the exact explanation of astrophysical BHs, such as Cygnus X-1, utilizing their deviation parameters from the Kerr BH [41–44]. Further, the astrophysical BHs might be inherently quantum objects, macroscopically different from the rotating ones predicted in Einstein's theory of gravity. Furthermore, the rotating H-BH may be a good candidate for studying how much quantum effects near the horizon can affect the radiation released from the BH system. The gravitational detections at LIGO [45–48], might be a clue for more efforts regarding the gravitational wave from the models of regular BHs. Recently, the upper bound thermally allowed in a head-on collision of two rotating H-BHs was found by using the numerical method [49]. The author of Ref. [49] showed how much the gravitational radiation is dependent on the parameters of the H-BH and found the effective range of the parameters using the data from GW150914 and GW151226 [45–48]. In this manner, the parameter g of the H-BH is treated as a universal constant in the spacetime, due to its relation to an energy level in the near horizon of the BH. According to [49], assuming that the mass of the first BH is unity and the second BH is smaller than the first one, one finds that a large value of g is not allowed and the possible upper bound of the parameter g ranges between 0.7 and 0.8. However, it needs more detection for the gravitational wave generated by a BH binary because the analysis becomes more precise in the limit of which a BH binary having a very small mass ratio. As another important observable aspect is a study of the gravitational lensing via regular BHs [50–52]. More recently, the authors in [53] investigated the observables of a strong deflection lensing, and estimated their values for the supermassive BH in the center of our Galaxy (Sgr A*). They have found that there is a very high resolution beyond our current stage which is needed to distinguish the modified H-BH from a Schwarzschild one.

It turns out to be a rather long process to solve Einstein's vacuum equations directly for a rotating solution. Instead, by describing a trick of Newman and Janis [54], one can obtain, for example, the Kerr solution from the Schwarzschild case. The same trick can then be applied to a regular case to achieve a rotating regular solution. In 2013, Bambi and Modesto [55] apply the Newman–Janis algorithm to the Hayward and to the Bardeen metrics to obtain a family of rotating regular BHs. In this paper, we first consider the most popular model of a regular BH derived in [4], namely the H-BH, and then study its radiating behavior and the resulting remnant by providing its Hawking temperature. We concisely study the dynamical stability of static spherically symmetric exact solutions in a self-gravitating NED theory via some conditions acting on the electromagnetic Lagrangian which lead to the linear stability for H-BHs solutions. In addition, the possibility of forming H-BHs at energy scales of a few TeVs is studied by obtaining their remnant mass. We compare different sizes of remnants with the noncommutative ones by including the noncommutative corrections in the line element of H-BH, i.e. the Noncommutative H-BH (NH-BH). Finally, using the Newman–Janis algorithm which is often remarked as a short cut to find spinning BH solutions via the corresponding non-rotating ones, we consider again the inspired noncommutativity and determine the Hawking temperature of the Noncommutative Rotating H-BH (NRH-BH). Throughout the paper, natural units are used, i.e. $\hbar = c = G = k_B = 1$ and Greek indices run from 0 to 3.

2. Hayward solution

The H-BH solution obtained by Hayward [4] is given by the following metric,

$$ds^2 = N(r)dt^2 - N^{-1}(r)dr^2 - r^2 d\Omega^2, \tag{1}$$

with

$$N(r) = 1 - \frac{2m(r)}{r} = 1 - \frac{2Mr^2}{r^3 + g^3}, \tag{2}$$

where g is a real free parameter and shows a positive constant measuring the deviations from the standard Kerr spacetime. In the above, the mass term $m(r) = \frac{Mr^3}{r^3+g^3}$ may show the mass inside the sphere of radius r such that in the limit $r \to \infty$ it approaches the BH mass M. This solution is everywhere nonsingular and the weak energy condition is not violated. The mass term $m(r)$ interpolates between the de Sitter core and the asymptotically flat infinity. The limits of large and small r of the metric function $N(r)$ are, respectively,

$$N(r) \approx 1 - \frac{2M}{r} + \frac{2Mg^3}{r^4}, \tag{3}$$

and

$$N(r) \approx 1 - \frac{2Mr^2}{g^3}, \tag{4}$$

which describes a central de Sitter solution, possibly in the regime where quantum gravity effects should appear. Such a metric has event horizons if $g^2 \leq \frac{8}{9}2^{\frac{1}{3}}M^2$. So, for a given value of M, quickly we find an upper bound for the Hayward parameter, i.e., $g \leq g^*$. For example if we set $M = 10$, there is a critical value for g, namely $g^* \approx 10.58$ that is the condition for having one degenerate event horizon which means for $g > g^*$ the horizons do not exist.

The emitted feature of such a regular BH can now be simply analyzed by displaying the temporal component of the metric as a function of radius for an extremal H-BH with different values of g. This has been presented in Fig. 1. This figure exhibits the possibility of having an extremal configuration with one degenerate event horizon at a minimal nonzero mass M_0. In fact, the condition for having one degenerate event horizon is that $M = M_0$ which means for $M < M_0$ there is no event horizon. The existence of a minimal nonzero mass may be interpreted as the de Sitter-like region corresponding to the interior of the horizon which yields a remnant that the H-BH may shrink to.

The horizon radius of the H-BH can be obtained by the real positive root of the following equation,

$$r_H^3 - 2Mr_H^2 + g^3 = 0. \tag{5}$$

So, one can find the H-BH mass in terms of r_H as follows:

$$M = \frac{r_H^3 + g^3}{2r_H^2}. \tag{6}$$

The numerical results of the mass versus the radius are presented in Fig. 2. As can be seen from Fig. 2, the minimal nonzero mass increases as the parameter g increases. The regularity at very short distances of the H-BH spacetime implies a remnant mass corresponding to a remnant radius r_0. Here we have shown that the final stage of the evaporation of H-BH is a remnant in which it has an increasing size with raising its own free parameter.

When such a regular BH radiates, its temperature is given by

$$T_H = \frac{1}{4\pi}\frac{dN(r)}{dr}\bigg|_{r=r_H} = \frac{Mr_H(r_H^3 - 2g^3)}{2\pi(r_H^3 + g^3)^2}. \tag{7}$$

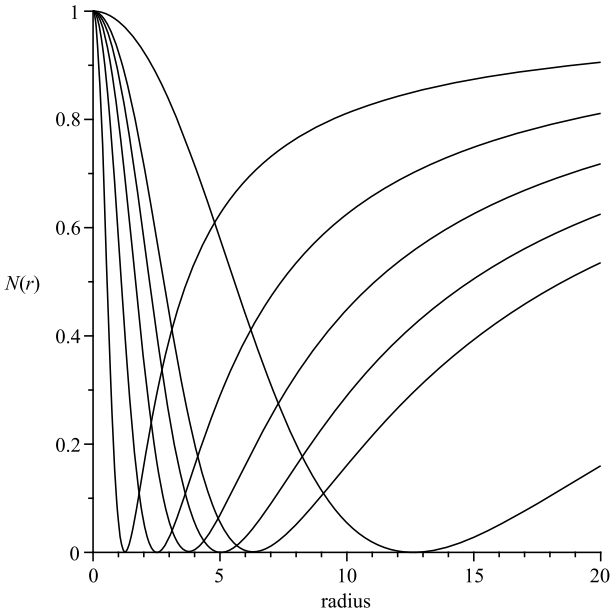

Fig. 1. The temporal component of the metric, $N(r)$, in terms of the radius r for different values of g. The figure displays the possibility of having extremal configuration with one degenerate event horizon at a minimal nonzero mass M_0. This presents the existence of M_0 such that the H-BH may shrink to. On the right-hand side of the figure, from top to bottom, the solid lines correspond to the H-BH for $g = 1.00$, 2.00, 3.00, 4.00, 5.00, and $g = 10.00$, respectively.

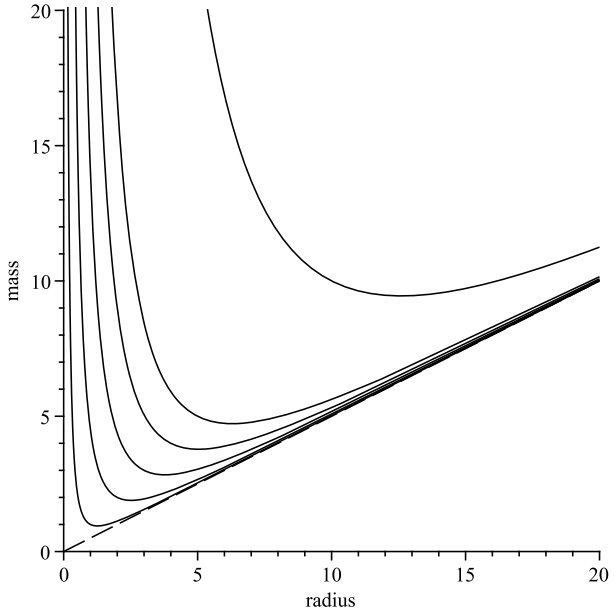

Fig. 2. The mass of the H-BH as a function of the horizon radius for different values of g. On the left-hand side of the figure, from left to right, the solid lines correspond to the H-BH for $g = 1.00$, 2.00, 3.00, 4.00, 5.00, and $g = 10.00$, respectively. The dashed line refers to the Schwarzschild case so that it corresponds to $g = 0$.

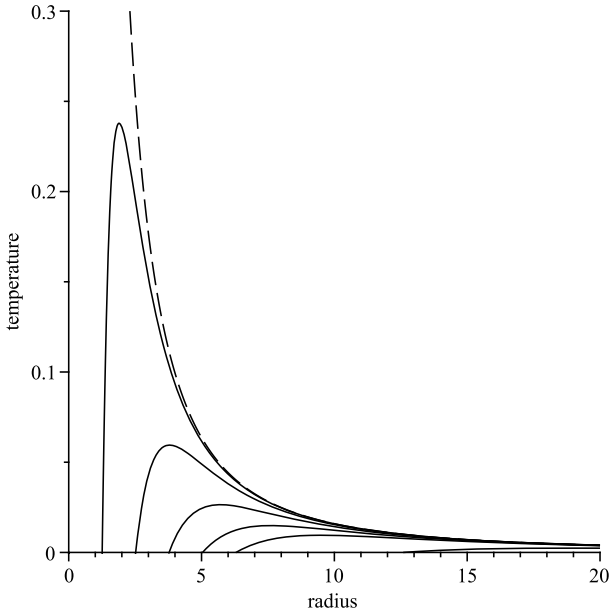

Fig. 3. The Hawking temperature versus the horizon radius. We have set $M = 10.00$. On the left-hand side of the figure, from left to right, the solid lines correspond to the H-BH for $g = 1.00, 2.00, 3.00, 4.00, 5.00$, and $g = 10.00$, respectively. The dashed line refers to the Schwarzschild case so that it corresponds to $g = 0$.

Due to the emission of Hawking radiation, the Hawking temperature finally reaches a peak at the final stage of the evaporation and then abruptly drops to zero so that a stable remnant is appeared. The remnant radius can be determined from $T_H = 0$, namely $r_0 = 2^{\frac{1}{3}} g$. This minimum radius corresponds to the remnant mass $M_0 = \frac{3}{2^{\frac{5}{3}}} g$.

The numerical result of the Hawking temperature in terms of the horizon radius is displayed in Fig. 3. According to Fig. 3, the temperature peak of the H-BH decreases as the parameter g increases, so a H-BH for a larger amount of g is colder and its remnant is bigger. If we set $g = 0$, so the Hawking temperature for the Schwarzschild BH, i.e. $T_H = \frac{M}{2\pi r_H^2}$, which is accompanied by a divergence at $M = 0$, is retrieved.

Table 1, for further specifications of the H-BH remnant, shows the numerical results of the remnant size, the remnant mass and also the maximum temperature for different values of g. In accordance with Table 1, as g becomes larger both the minimal mass and the minimal radius get larger but the temperature peak becomes smaller. In the limit $g \gg 1$, the free parameter g is proportional to the remnant mass and to the remnant radius, i.e. $g \propto M_0 \propto r_0$. In other words, for an adequately large amount of g which corresponds to a large radius, there is a linear relationship between the minimal mass and the minimal radius which is similar to the result appeared in the relationship between the horizon radius and the BH mass for the Schwarzschild BH.

Here we would like to check the thermodynamical stability of the H-BH. The thermodynamic stability of a system can be investigated in different ensembles. In the canonical ensemble, the thermal stability of a system is determined by the sign of its heat capacity. The positivity of the heat capacity is sufficient to ensure thermal stability of a thermodynamical system. So, a BH is thermodynamically unstable when its heat capacity is negative. The heat capacity of the BH

Table 1
The remnant mass, the remnant radius and also the maximum temperature of the H-BH for different values of g. As the parameter g increases the size and the mass of the H-BH remnant increase but the maximum temperature decreases. For a large amount of g, i.e. $g \gg 1$, there is a linear relationship between the remnant mass and the remnant radius. As can be seen from the table, the results are confirmed by the numerical results of Figs. 1, 2 and 3.

H-BH			
Free parameter	Remnant mass	Remnant radius	Maximum temperature
$g = 1.00$	$M_0 \approx 0.94$	$r_0 \approx 1.26$	$T_H(max) \approx 0.238$
$g = 2.00$	$M_0 \approx 1.89$	$r_0 \approx 2.52$	$T_H(max) \approx 0.059$
$g = 3.00$	$M_0 \approx 2.83$	$r_0 \approx 3.78$	$T_H(max) \approx 0.026$
$g = 4.00$	$M_0 \approx 3.78$	$r_0 \approx 5.04$	$T_H(max) \approx 0.015$
$g = 5.00$	$M_0 \approx 4.72$	$r_0 \approx 6.30$	$T_H(max) \approx 0.009$
$g = 10.00$	$M_0 \approx 9.45$	$r_0 \approx 12.60$	$T_H(max) \approx 0.002$

can be obtained using $C = \frac{\partial M}{\partial r_H}\left(\frac{\partial T_H}{\partial r_H}\right)^{-1}$. For $M > M_0$, we have $\frac{\partial M}{\partial r_H} > 0$ (see Fig. 2). Thus the sign of the heat capacity will be determined by the sign of $\left(\frac{\partial T_H}{\partial r_H}\right)^{-1}$ (see Fig. 3). There is a stable region of positive heat capacity, which represents the near-horizon thermodynamics. In this region, the temperature reaches a maximum value of its amount at the position that the slope of the temperature curve is zero, i.e. $\frac{\partial T_H}{\partial r_H} = 0$, then the heat capacity becomes singular for this special value, known as Davies' point, where the temperature is maximum and the heat capacity changes from negative infinity to positive infinity [56,57]. In this point the whole thermodynamic process separates into two stages; the early stage with a positive heat capacity and the late stage with a negative heat capacity. Indeed, this is the process from an initial unstable large BH to a final stable extremal BH.

It is obvious that an asymptotically flat uncharged BH is thermally unstable, so in order to achieve a stable BH, one can add the cosmological constant, the electric charge or the magnetic charge to the solutions. In the next section, we briefly review a special theory of NED, which predicts a recognizable physical source for the central regularity of the H-BH, and indicate an exact solution for the H-BH to analyze its stability in the NED theory.

3. Stability analysis in an exact regular BH solution in Einstein-nonlinear electrodynamics

It has been shown that general relativity coupled to NED yields the nontrivial spherically symmetric solutions with a globally regular metric [15–18]. The H-BH is also an exact solution obtained in the Einstein gravity coupled with NED [25]. In this section, we briefly study the H-BH in NED and show its stability under linear perturbations. Stability properties in self-gravitating NED were investigated by Moreno and Sarbach [58]. They found adequate criteria for the linear stability with respect to arbitrary linear fluctuations in the metric and in the gauge potential. These criteria are in the form of inequalities to be fulfilled by the NED Lagrangian density and its derivatives.

The action describing the dynamics of a self-gravitating NED field in general relativity is

$$S = \frac{1}{4\pi}\int\left(\frac{R}{4} - L(F)\right)\sqrt{-\mathsf{g}}d^4x, \tag{8}$$

where R is the Ricci scalar with respect to the spacetime metric $\mathsf{g}_{\alpha\beta}$, and the Lagrangian density $L(F)$ denotes a nonlinear function of the Lorentz invariant $F = \frac{1}{4}F_{\alpha\beta}F^{\alpha\beta}$, where $F_{\alpha\beta} = \partial_\alpha A_\beta -$

$\partial_\beta A_\alpha$ is the electromagnetic field. The Lagrangian density is an arbitrary function which leads to $L(F) \approx F$ at small F, i.e. for the weak field limit, describes the Maxwell theory. The temporal component of Einstein equations, ${G_0}^0$, resulting from the above action yields

$$m(r) = \int L(F) r^2 dr. \tag{9}$$

Substituting $m(r)$ into a static and spherically symmetric configuration one finally finds the Hayward metric [25].

For the stability analysis, it is convenient to consider the Lagrangian density to be a function of the dimensionless variable $y = \sqrt{2g^2F} = \frac{g^2}{r^2}$. Note that the parameter g here is not just a universal constant, but a magnetic charge associated with a physically reasonable matter content. The H-BH which does have a correct weak field limit is obtained from the Lagrangian density

$$L(y) = \frac{3}{2sg^2} \frac{y^3}{(1+y^{\frac{3}{2}})^2}, \tag{10}$$

where $s = \frac{|g|}{2M}$ is a positive constant. The metric function N in terms of y is given by

$$N = 1 - \frac{1}{s} \frac{y^{\frac{1}{2}}}{1+y^{\frac{3}{2}}}. \tag{11}$$

The equation $N(y_m, s) = 0$ is solved by the single root $s = s_c = \frac{2^{\frac{2}{3}}}{3}$, where $y_m = 2^{-\frac{2}{3}}$ is a single minimum of N. At y_m, for $s < s_c$ the minimum of N is negative, for $s = s_c$ the minimum vanishes and for $s > s_c$ the minimum is positive. In other words, for $g^2 < 4M^2 s_c^2 = \frac{8}{9} 2^{\frac{1}{3}} M^2$ we have two event horizons, for $g^2 = \frac{8}{9} 2^{\frac{1}{3}} M^2$ the horizons shrink into a single one (extremal BH), and no event horizon for $g^2 > \frac{8}{9} 2^{\frac{1}{3}} M^2$.

According to [58] (see also [59]), one can conclude that the linear stability criteria on the corresponding BH solutions obligates the satisfaction of the following inequalities

$$\begin{aligned} &L > 0, \\ &L_{,y} = \frac{9}{2sg^2} \frac{y^2}{(1+y^{\frac{3}{2}})^3} > 0, \\ &L_{,yy} = \frac{9}{4sg^2} \frac{4y - 5y^{\frac{5}{2}}}{(1+y^{\frac{3}{2}})^4} > 0, \\ &3L_{,y} \geq y N L_{,yy}, \end{aligned} \tag{12}$$

where $L_{,y}$ and $L_{,yy}$ are the first and second derivatives of L with respect to y, respectively. The last inequality above can also be written as

$$3 \geq N f(y) > 0, \tag{13}$$

where the function $f(y)$ is defined as

$$f(y) = \frac{y L_{,yy}}{L_{,y}} = \frac{4 - 5y^{\frac{3}{2}}}{2(1+y^{\frac{3}{2}})}. \tag{14}$$

The function $f(y)$ is smoothly lessening with $f(0) = 2$. Also, since the metric function has a single minimum at $2^{-\frac{2}{3}}$, therefore one has $y_H \leq 2^{-\frac{2}{3}}$, where y_H is the value of y at the event horizon. Accordingly, it is easy to check that the conditions (12) for all $0 \leq y \leq y_H$, are satisfied and so Hayward BHs are stable.

4. Higher-dimensional Hayward solution

In the continuing search for quantum gravity, the BH thermodynamics may be associated with future experimental results at the LHC [60–62]. For example, the semiclassical analysis of loop quantum BHs prepares regular BHs without singularity such that their minimum sizes are at the Planck scale regime [63]. As another example, gravity's rainbow motivated by doubly special relativity, using the modified dispersion relation [64], produces remnants at the final phase of the BH evaporation. As an important note, the thermodynamics descriptions of H-BHs are substantially similar to that of the framework of gravity's rainbow [65]. In the context of gravity's rainbow [66], the remnant mass has found to be greater than the energy scale at which experiments were performed at the LHC. In this section, we shall extend our study into extra dimensions to investigate the phenomenological implications on the production of BHs at TeV scales.

The metric (1) can be generalized to a higher-dimensional spacetime. Considering static, spherically symmetric d-dimensional spacetime one obtains [67]

$$ds^2 = Ndt^2 - N^{-1}dr^2 - r^2 d\Omega_{d-2}^2, \tag{15}$$

with

$$N = N(r, r_g) = 1 - \frac{r_g^{d-3} r^2}{r^{d-1} + g_d^3}, \tag{16}$$

where $g_d = r_g^{\frac{d-3}{3}} l^{\frac{2}{3}}$ is Hayward's parameter in the higher dimensional spacetime and depends on the extra dimension models. The parameter r_g is the gravitational radius of the H-BH in extra dimensions in which at far distance it reproduces its correct Schwarzschild asymptotic form in the 4-dimensional case, i.e. $2M$. The parameter l is a length-scale parameter. One of the main assumptions here is that there is a critical energy Λ and the corresponding length-scale parameter l in such a way that one has $l = \Lambda^{-1}$. This takes account of the fact that the metric should be modified when the spacetime curvature becomes comparable with l^{-2}. On the other hand one can use a classical solution obtained by the effective action of the modified gravity. This means that the Planck length-scale, where quantum gravity effects become significant, is much smaller than the critical scale parameter l. Thus, it is reasonable to assume that the critical energy scale Λ to be as small as a TeV in order to solve the hierarchy problem [68–72]. This is supported by the fact that most of the phenomenological studies of a viable fundamental theory have presumed that the absolute maximal value of the curvature is restricted by some fundamental value such that its corresponding characteristic energy cannot lie far above the TeV scale [66,73–76]. Hence, we assume $l \sim 1$ TeV^{-1}. However, in a general case, l is a parameter of the corresponding UV complete theory including parameters such as mass (and/or charge), which specify a concrete solution [67].

For $g = 0$, the line element (15) reproduces the Tangherlini solution of the Einstein equations. For $d = 4$, one has $g_d = g = (2Ml^2)^{\frac{1}{3}}$ and therefore the metric (15) reduces to (1). The limits of large and small r of the metric function N are, respectively,

$$N \approx 1 - \left(\frac{r_g}{r}\right)^{d-3}, \tag{17}$$

and

Table 2
The remnant mass of the higher dimensional H-BH (∼ TeV) for different number of spacetime dimensions d and several values of g_d. As the parameter g_d increases the mass of the BH remnant increases but by increasing the spacetime dimensions the remnant mass decreases.

d	Higher dimensional H-BH remnant		
	M_0; $g_d = 1$	M_0; $g_d = 5$	M_0; $g_d = 10$
4	0.94	4.72	9.45
5	0.71	2.36	3.98
6	0.62	1.64	2.49
7	0.59	1.31	1.85
8	0.56	1.12	1.51
9	0.55	1.00	1.30
10	0.54	0.92	1.16
11	0.53	0.86	1.06

$$N \approx 1 - \left(\frac{r_g^{d-3}}{g_d^3}\right) r^2. \tag{18}$$

These satisfy the limiting metric conditions. The critical value of the gravitational radius r_g^* can be determined by conditions $N(r^*) = N'(r^*) = 0$ as follows:

$$r_g^* = \left(\frac{d-1}{d-3}\right)^{\frac{1}{2}} \left(\frac{d-1}{2}\right)^{\frac{1}{d-3}} l, \tag{19}$$

where the prime abbreviates $\frac{d}{dr}$. For $r_g > r_g^*$ the line element (15) has two horizons, while for $r_g < r_g^*$ there is no event horizon.

The Hawking temperature of the H-BH in d dimensions takes the form

$$T_H = \frac{r_g^{d-3}}{4\pi} \frac{(d-3)r^d - 2g_d^3 r}{(r^{d-1} + g_d^3)^2}. \tag{20}$$

The temperature vanishes in the limit $r \to r_0$ such that for $r < r_0$, the temperature has no physical meaning. The remnant radius r_0 is found to be

$$r_0 = \left(\frac{2g_d^3}{d-3}\right)^{\frac{1}{d-1}}. \tag{21}$$

This minimum horizon radius implies a remnant mass as follows:

$$M_0 = \frac{1}{2}\left(\frac{d-1}{4^{\frac{1}{d-1}}}\right)^{\frac{1}{d-3}} \left(\frac{g_d^3}{d-3}\right)^{\frac{1}{d-1}}. \tag{22}$$

Here, we assume that the critical energy scale Λ is at around the electroweak scale, i.e. ∼ TeV. We present the results given in Table 2. We see that as g_d grows the remnant mass increases, while as the number of spacetime dimension d becomes larger the remnant mass decreases. Table 2 clearly shows that, for a large number of extra dimensions, the energy scale of the minimal mass is sufficient for the energy scale of the current runs of the LHC. As a result, if extra dimensions do exist and if the number of spacetime dimensions becomes sufficiently large with a sufficiently small Λ ($\Lambda \sim 1$ TeV), then the possible formation and detection of BHs in TeV-scale collisions at the LHC will be enhanced.

5. Noncommutative Hayward solution

Our strategy here is that, firstly, the noncommutativity influences on the spacetime of non-rotating Hayward are investigated and the thermodynamics features of the NH-BH are determined. Afterwards, in the later section, taking into account the Newman–Janis algorithm, we apply the inspired noncommutativity and recompute the Hawking temperature of the NRH-BH.

In accord with [77], the Newman–Janis algorithm works only for vacuum solutions but the authors in [78] have presented a new prescription that comprises the case of non-vanishing stress tensors. As an introduction of the idea, let us begin by the Schwarzschild-like form of spacetimes which explain the line elements in the so-called Kerr–Schild classification and in the presence of matter

$$ds^2 = ds_M^2 - \frac{h(r)}{r^2}\left(n_\alpha dx^\alpha\right)^2, \tag{23}$$

where the expression ds_M^2 is the Minkowski metric in a spherical basis and n_α is a null vector in the coordinates of Minkowski. The function $h(r)$ can be written as

$$h(r) = 2m(r)r. \tag{24}$$

In accordance with the Kerr–Schild decomposition, Eq. (24) has a generic validity, thus its general form is unchanged and it is not sensitive to various structures of the mass term. The expression $h(r)$ for the H-BH metric is given by

$$h(r) = \frac{2Mr^4}{r^3+g^3}. \tag{25}$$

Here, we apply the inspired noncommutative methodology [35–39] (see also [79]). According to this method, the point-like structure of mass, instead of being entirely localized at a point, is characterized by a smeared structure throughout a region of linear size $\sqrt{\theta}$. This means that the mass density of a static, spherically symmetric, particle-like gravitational source cannot be a delta function distribution, but will be found to be a Gaussian distribution

$$\rho_\theta(r) = \frac{M}{(4\pi\theta)^{3/2}} e^{-\frac{r^2}{4\theta}}. \tag{26}$$

The smeared mass distribution can implicity be written in terms of the lower incomplete Gamma function,

$$M_\theta = \int_0^r \rho_\theta(r) 4\pi r^2 dr = \frac{2M}{\sqrt{\pi}}\gamma\left(\frac{3}{2}; \frac{r^2}{4\theta}\right). \tag{27}$$

The resulting metric describing the NH-BH is given by Eq. (1), with the following $m(r)$ in terms of the smeared mass distribution M_θ

$$m(r) = M_\theta\left(\frac{r^3}{r^3+g^3}\right). \tag{28}$$

The thermodynamics description of the NH-BH can now be simply analyzed by displaying the temporal component of the metric versus the radius for an extremal BH with different values of g which has been presented in Fig. 4.[1]

[1] For simplicity of numerical calculations, we assume $\theta = 1$.

It is clear that the metric of the NH-BH has a coordinate singularity at the event horizon as

$$r_H = 2m(r_H), \tag{29}$$

with

$$m(r_H) = \frac{2M}{\sqrt{\pi}} \left(\frac{r_H^3}{r_H^3 + g^3} \right) \gamma \left(\frac{3}{2}; \frac{r_H^2}{4\theta} \right). \tag{30}$$

The analytical solution of Eq. (29) for the horizon radius in a closed form is not feasible, but one can solve it to obtain M, which gives the mass of the NH-BH in terms of r_H. We find

$$M = \frac{r_H^3 + g^3}{2r_H^2 \left[\mathcal{E}\left(\frac{r_H}{2\sqrt{\theta}} \right) - \frac{r_H}{\sqrt{\pi\theta}} e^{-\frac{r_H^2}{4\theta}} \right]}, \tag{31}$$

where $\mathcal{E}(n)$ is the Gaussian error function defined as $\mathcal{E}(n) \equiv \frac{2}{\sqrt{\pi}} \int_0^n e^{-x^2} dx$. In the limit $\theta \to 0$, the Gaussian error function is equal to one and the exponential term is reduced to zero, thus we recover Eq. (6). In other words, if $\sqrt{\theta}$ is too small, the background geometry is interpreted as a smooth differential manifold and the smeared-like mass descends to the point-like mass. However, in the regime that noncommutative fluctuations are important, $r \to \sqrt{\theta}$, the microstructure of spacetime deviates considerably from the macroscopic one and provides new physics at very short distances.

The results of the numerical solution of the mass as a function of the horizon radius are displayed in Fig. 5. According to the numerical results it is concluded that the noncommutative version of the mass equation (31), leads to a bigger minimal nonzero mass at small radii in comparison with the standard commutative version.

The Hawking temperature of the NH-BH can be written as

$$T_H = \frac{M}{4\sqrt{(\pi\theta)^3}\left(r_H^3 + g^3\right)^2} \Bigg[4r_H \sqrt{\pi\theta^3} \left(\frac{r_H^3}{2} - g^3 \right) \mathcal{E}\left(\frac{r_H}{2\sqrt{\theta}} \right) - r_H^2 e^{-\frac{r_H^2}{4\theta}} \times \left(r_H^5 + 2r_H^3\theta + r_H^2 g^3 - 4\theta g^3 \right) \Bigg]. \tag{32}$$

In the commutative version and for $g = 0$, the Gauss error function is unity and the exponential term is zero, so we retrieve the Hawking temperature of a Schwarzschild BH. The numerical result of the NH-BH temperature in terms of the horizon radius is shown in Fig. 6. From the figure we see that the maximum temperature decreases with raising the parameter g. As a result, the size and the mass of the NH-BH remnant at the ultimate phase of the evaporation is bigger in comparison with the noncommutative Schwarzschild one.

For more specifications, we present Table 3 that is similar to Table 1. From Table 3 we see that as g grows both the remnant mass and the remnant radius are increased which finally, in the limit $g \gg 1$, yields a proportional relationship $g \propto M_0 \propto r_0$. A comparison between the final stages of the evaporation for the noncommutative Schwarzschild BH and the NH-BH shows that raising the size and the mass of the remnant and also getting a colder BH is affected by an increase in the parameter g. In addition, as can be seen from Figs. 4, 5, 6 and Table 3 the noncommutative coordinates yields a bigger remnant and also a colder BH at small radii compared to its commutative case.

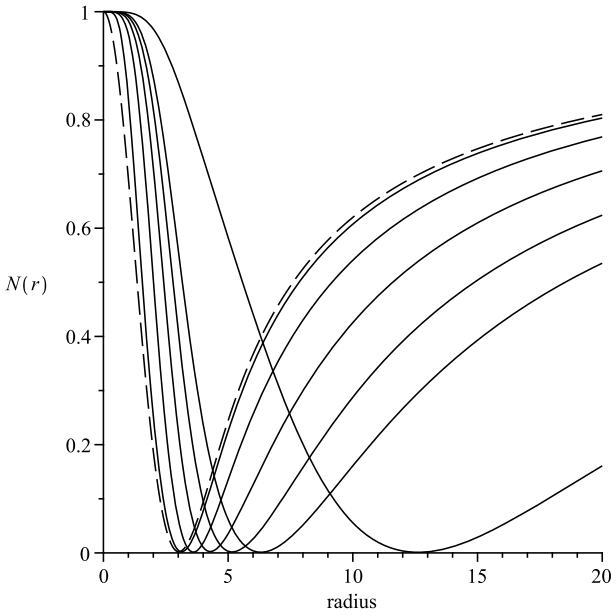

Fig. 4. The temporal component of the metric, versus the radius for different values of g. The figure shows the possibility of having extremal configuration with one degenerate event horizon at $M = M_0$ (extremal NH-BH). This shows the existence of a minimal non-zero mass that the BH can shrink to. On the right-hand side of the figure, from top to bottom, the solid lines correspond to the NH-BH for $g = 1.00,\ 2.00,\ 3.00,\ 4.00,\ 5.00$, and $g = 10.00$, respectively. The dashed line refers to the Schwarzschild case so that it corresponds to $g = 0$.

Table 3
The table in the upper place shows the remnant mass, the remnant radius and the maximum temperature of the noncommutative Schwarzschild BH, while the table below shows them for the NH-BH with different values of g.

Noncommutative Schwarzschild BH			
Remnant mass		Remnant radius	Maximum temperature
$M_0 \approx 1.90$		$r_0 \approx 3.02$	$T_H(max) \approx 0.065$
NH-BH			
Free parameter	Remnant mass	Remnant radius	Maximum temperature
$g = 1.00$	$M_0 \approx 1.96$	$r_0 \approx 3.13$	$T_H(max) \approx 0.062$
$g = 2.00$	$M_0 \approx 2.31$	$r_0 \approx 3.60$	$T_H(max) \approx 0.045$
$g = 3.00$	$M_0 \approx 2.95$	$r_0 \approx 4.28$	$T_H(max) \approx 0.026$
$g = 4.00$	$M_0 \approx 3.79$	$r_0 \approx 5.16$	$T_H(max) \approx 0.015$
$g = 5.00$	$M_0 \approx 4.72$	$r_0 \approx 6.31$	$T_H(max) \approx 0.009$
$g = 10.00$	$M_0 \approx 9.45$	$r_0 \approx 12.60$	$T_H(max) \approx 0.002$

According to our results, for $g < 5$ the minimum required energy for the formation of NH-BHs at particle colliders such as LHC will be larger compared to the H-BH case. This is indeed a consequence of noncommutative effects and may be interpreted as an indication of a suppression of the BH production arisen from the local fluctuations of the geometry at short distances. This is in agreement with the results obtained in the context of gravity's rainbow [66]. The authors in Ref. [66] have proposed this as a possible explanation for the absence of BHs at the LHC.

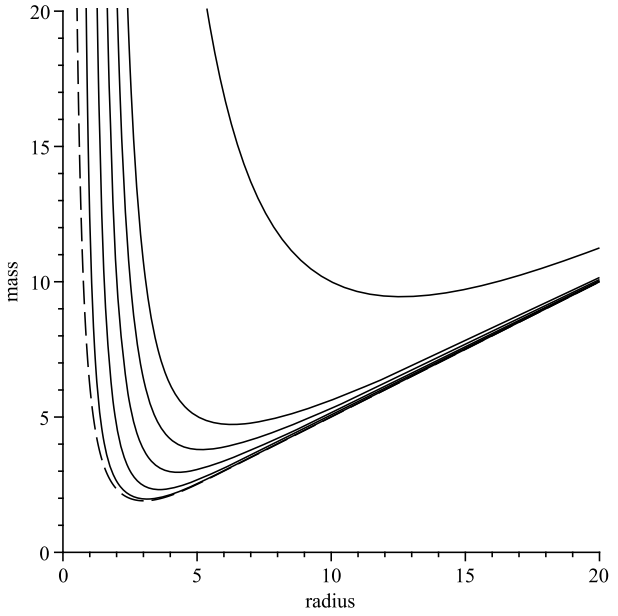

Fig. 5. The mass of the NH-BH versus the horizon radius for different values of g. On the left-hand side of the figure, from left to right, the solid lines correspond to the NH-BH for $g = 1.00$, 2.00, 3.00, 4.00, 5.00, and $g = 10.00$, respectively. The dashed line refers to the Schwarzschild case so that it corresponds to $g = 0$.

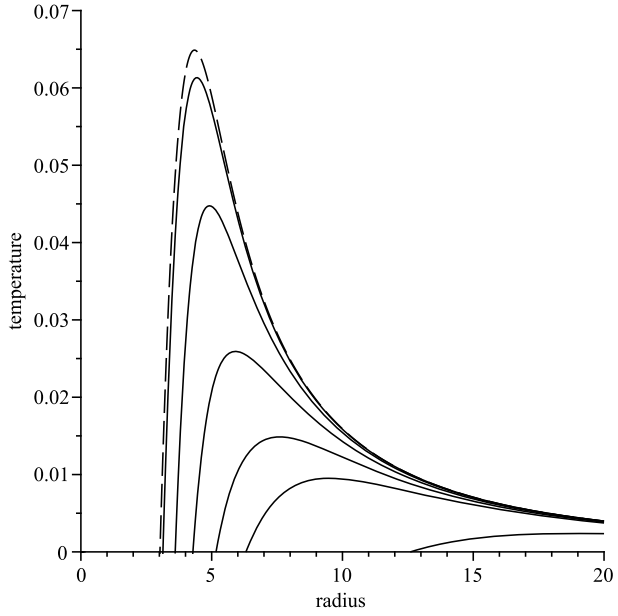

Fig. 6. The Hawking temperature versus the horizon radius. We have set $M = 10.00$. On the left-hand side of the figure, from left to right, the solid lines correspond to the NH-BH for $g = 1.00$, 2.00, 3.00, 4.00, 5.00, and $g = 10.00$, respectively. The dashed line refers to the Schwarzschild case so that it corresponds to $g = 0$.

In addition, they have found that a remnant depends critically on the structure of the rainbow functions [80]. They have argued that, using the framework of gravity's rainbow, a remnant is formed for all black objects in such a way that it is a model-independent phenomenon.

Given that the physical behavior of the H-BH is qualitatively the same with or without noncommutativity, one might ask the question "is there any reason to introduce a smearing of the source and/or the Hayward's parameter?". In order to answer this question we should explain that the temperature is considerably different and is lower in the case of the noncommutativity. By changing noncommutative's parameter and keeping the Hayward's parameter to be constant, the results are qualitatively similar. Nevertheless, in principle, there are two good reasons to show that there are fundamental differences between two cases. First, the spacetime noncommutativity does not depend on the curvature, but is an intrinsic property of the manifold itself even in the absence of gravity which is denoted by the parameter θ and can eliminate some kind of divergences which appear in general relativity. Hence, if any effect is produced by the noncommutativity it must appear also in weak fields. Second, the concept of "weak" or "strong" field is sensible only if one compares the field strength with a proper scale. In the gravitation theory, we have a natural and unique scale, that is the Planck scale. Therefore, the gravitational field strength can still be considered "weak" even near a BH, with respect to the Planck scale. This issue justifies the adoption of linearized field equations as a temporary laboratory to test the effect of noncommutativity until the horizon radius is larger than the Planck length [81].

From the other point of view, the H-BH is a regular solution of a modified Einstein equation, and it is also found in the Einstein gravity coupled with NED. It is well-known that in the near horizon of a BH, the quantum effect becomes important because of the strong gravity, therefore the geometry of the spacetime can be modified from the quantum effect at the near horizon and the intrinsic singularity inside the BH can be eliminated. One could expect that the metric of the BH is modified in the near horizon region due to the quantum effect. The extent of the deviation from the standard solution of Einstein equations is denoted by the free parameter g. Hence, the parameter g can describe how much the quantum effect near the horizon affects the deviation from the standard energy level and the radiation. Along this line of reasoning we take them as two distinct situations.

For further specifications, the numerical result of the temperature in terms of the horizon radius for the noncommutative Schwarzschild and Hayward BHs are shown in Figs. 7 and 8, respectively. We just change the value of θ for $g = 0$. From the figures we see that the maximum temperature decreases considerably with increasing the parameter θ compared to the results obtained just by tuning g. As a result, the size and the mass of the NH-BH remnant at the ultimate phase of the evaporation is bigger for small amounts of θ, while is smaller for large amounts of θ in comparison with the case that we change the Hayward's parameter and keeping θ equal to zero. In fact, noncommutative's parameter is more sensitive to small radii, while Hayward's parameter has a linear relationship with the remnant radius.

It may be noted that as another striking example of regular BHs, if the Bardeen solution is chosen, solely the mass term will be changed, however the general properties will be directed to entirely comparable consequences to those above [82].

6. Noncommutative rotating Hayward solution

For spinning solution, we apply the Newman–Janis algorithm, and assuming that the mass term $m(r)$ is not affected by the complexification $r \to r' = r + ia\cos\vartheta$, the general form of the Kerr–Schild decomposition (23) holds

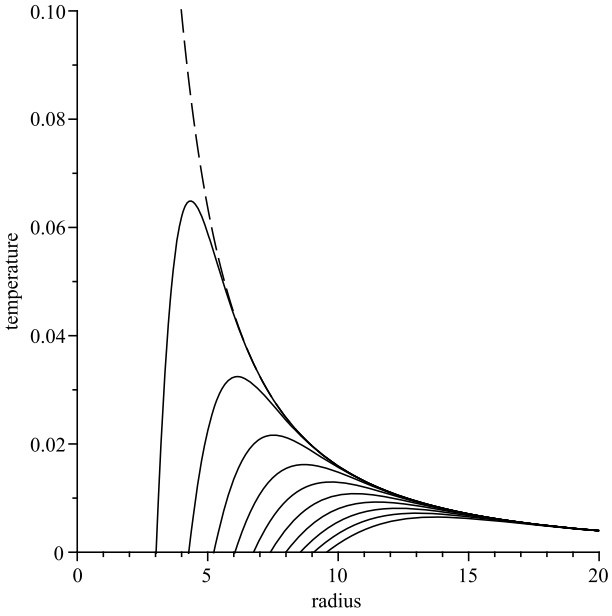

Fig. 7. The Hawking temperature versus the horizon radius. We have set $M = 10.00$. On the left-hand side of the figure, from left to right, the solid lines correspond to the noncommutative Schwarzschild BH for $\theta = 1.00, 2.00, 3.00, \ldots, 10.00$, respectively. The dashed line refers to the commutative Schwarzschild BH so that it corresponds to $\theta = 0$.

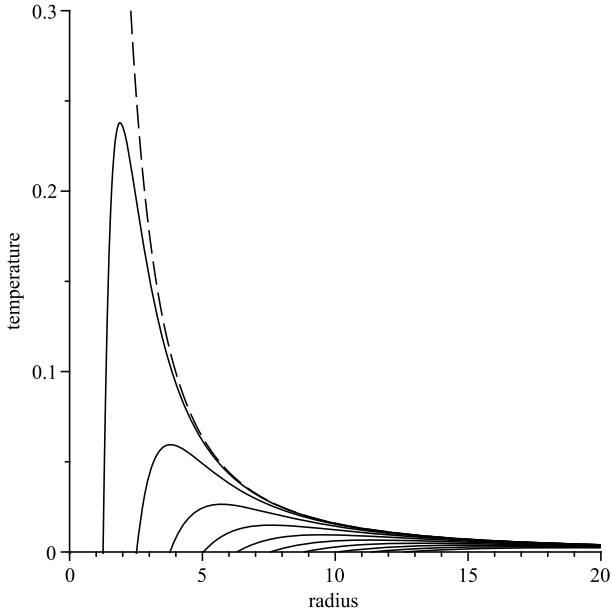

Fig. 8. The Hawking temperature versus the horizon radius. We have set $M = 10.00$. On the left-hand side of the figure, from left to right, the solid lines correspond to the H-BH for $g = 1.00, 2.00, 3.00, \ldots, 10.00$, respectively. The dashed line refers to the Schwarzschild BH so that it corresponds to $g = 0$.

$$ds^2 = ds_M^2 - \frac{h(r)}{r'\bar{r}'}\left(n_\alpha dx^\alpha\right)^2, \tag{33}$$

where n_α is written in spheroidal coordinates and $h(r)$ is unaltered by expressing $m(r')$ as $m(\mathrm{Re}(r')) = m(r)$. In fact, even with changing the symmetry from a spherically symmetric geometry to an axially symmetric geometry, the formal structure of the Kerr–Schild solution does not change. This is consistent with the solution of type-I or the first-class solution of the RH-BH in [55], i.e. the complexification of the $\frac{1}{r}$ term as in Schwarzschild, without changing the mass term.

Now, with the above explanation, one can obtain the line element of RNH-BH in Boyer–Lindquist coordinates

$$\begin{aligned} ds^2 = {} & \frac{\Delta - a^2\sin^2\vartheta}{\Sigma}dt^2 - \frac{\Sigma}{\Delta}dr^2 - \Sigma d\vartheta^2 + 2a\sin^2\vartheta\left(1 - \frac{\Delta - a^2\sin^2\vartheta}{\Sigma}\right)dtd\phi \\ & - \sin^2\vartheta\left[\Sigma + a^2\sin^2\vartheta\left(2 - \frac{\Delta - a^2\sin^2\vartheta}{\Sigma}\right)\right]d\phi^2, \end{aligned} \tag{34}$$

where $\Delta := r^2 - 2m(r)r + a^2$ (with $m(r)$ given by Eq. (28)) and $\Sigma := r^2 + a^2\cos^2\vartheta$.

The Hawking temperature of the NRH-BH is then found to be

$$\begin{aligned} T_H &= \frac{1}{4\pi(r_+^2 + a^2)}\frac{d\Delta}{dr}\bigg|_{r=r_+} \\ &= -\frac{1}{4\sqrt{(\pi\theta)^3}(r_+^3 + g^3)^2(r_+^2 + a^2)}\Bigg[8\sqrt{\pi\theta^3}Mr_+^3\left(\frac{r_+^3}{4} + g^3\right)\mathcal{E}\left(\frac{r_+}{2\sqrt{\theta}}\right) \\ &\quad + \left(Mr_+^9 - 2M\theta r_+^7 + Mg^3r_+^6 - 8M\theta g^3 r_+^4\right)e^{-\frac{r_+^2}{4\theta}} \\ &\quad - 2\sqrt{\pi\theta^3}r_+(r_+ + g)^2(r_+^2 - gr_+ + g^2)^2\Bigg]. \end{aligned} \tag{35}$$

Note that, for the commutative case and for $g = a = 0$, the function $\mathcal{E}\left(\frac{r_+}{2\sqrt{\theta}}\right)$ becomes one and the exponential term is zero, but the last term in Eq. (35) which is independent of the mass M will be reduced to $\frac{1}{2\pi r_+}$. Hence, one retrieves the standard result

$$T_H = -\frac{M}{2\pi r_+^2} + \frac{1}{2\pi r_+} = \frac{1}{4\pi r_+}, \tag{36}$$

where in this case $r_+ = r_H = 2M$. Finally, the numerical result of the Hawking temperature as a function of the outer horizon radius (Eq. (35)) is shown in Fig. 9. In accord with the figure, the size and the mass of the NRH-BH remnant at the final stage of the evaporation increase with increasing the parameter g. However, in the rotating case it is not so sensitive to g with respect to the non-rotating one.

In order to compare the noncommutative results with the commutative case ($\theta \to 0$), we display the plot for the temperature of the RH-BH as a function of r_+ (see Fig. 10). One can see that the noncommutative effects are caused to have a larger size and mass of the remnant in addition to a colder BH. Furthermore, it is reasonable to expect that the enlarging the amounts of the remnant mass is the role of the rotation as well.

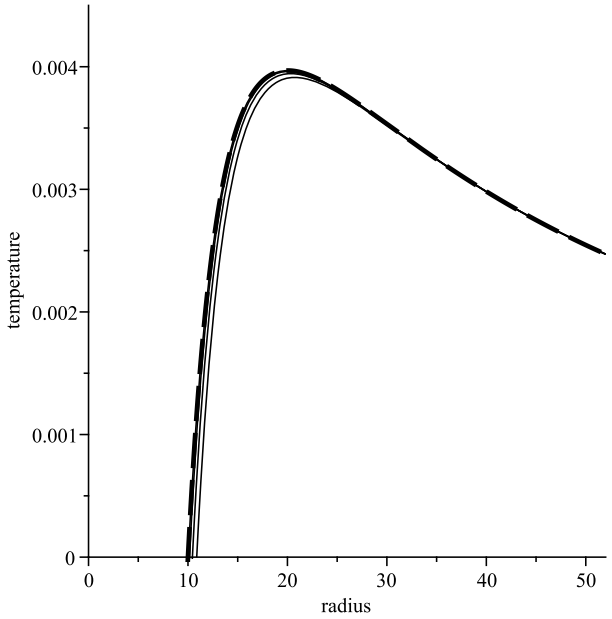

Fig. 9. The temperature T_H versus the outer horizon radius, r_+. We have set $M = 10.00$ and $a = 1.00$. On the left-hand side of the figure, from left to right, the solid lines correspond to the NRH-BH for $g = 1.00$, 2.00, 3.00, 4.00, 5.00, and $g = 10.00$, respectively. The dashed line refers to the noncommutative Kerr BH so that it corresponds to $g = 0$. It is clear that the curves are not so sensitive to g.

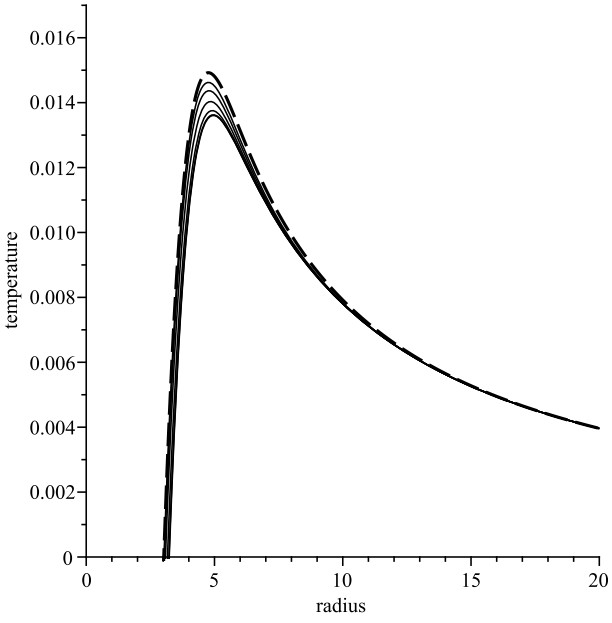

Fig. 10. The temperature T_H versus the outer horizon radius, r_+. We have set $M = 10.00$ and $a = 1.00$. The solid lines through the center of the figure, from top to bottom, correspond to the RH-BH for $g = 1.00$, 2.00, 3.00, 4.00, 5.00, and $g = 10.00$, respectively. The dashed line refers to the Kerr BH so that it corresponds to $g = 0$.

Generally, in Figs. 9 and 10, we see that the feature of the temperature is nearly similar to that of the nonrotating case. After a temperature peak, the NRH-BH calms down to a zero temperature as a NRH-BH remnant at the final phase of its evaporation. The size and the mass of this remnant become larger with respect to the nonrotating solution and this is due to the fact that the rotational kinetic energy is kept in the final format. As a consequence, the noncommutative effects and the rotation factor can raise the minimum value of energy for the possible production of BHs in TeV-scale collisions at particle colliders, so that the possibility for the formation and detection of BHs would be reduced.

7. Summary

We have proposed that the final phase of the BH evaporation is a stable remnant. In this study, the H-BH as a most popular model of regular BHs has been chosen. We have verified that the exact H-BH solution extracted from the theory of NED coupled with gravity satisfies sufficient conditions for the linear stability with respect to arbitrary linear fluctuations. The thermodynamics features of its non-rotating and rotating solution in the presence of an inspired model of noncommutative geometry have been analyzed. The effect of this inspired noncommutativity in the microscopic feature of spacetime is that all point structures are replaced by structures smeared via such an inspired microstructure. We have explored the effect that the deformation of a point mass has on the thermodynamics of H-BH solutions. Thus, the corrections to the Hawking temperature via such a modification of the theory have been found. Finally we have extended our analysis to the thermodynamic properties of noncommutative spinning solutions, providing their Hawking temperature. It is concluded that, the noncommutative effects cause an increasing size and mass of the remnant and also making the BH to be colder in the small radii regime as the free parameter g increases. As a result, the noncommutative effects can enhance the minimum required energy for the creation of such BHs in the present experimental attempts at the LHC. This may reduce the possibility for the formation and detection of BHs in TeV-scale collisions at particle colliders. However, if we have enough chance to have large extra dimensions, then it may make the BH production experimentally accessible at colliders.

Acknowledgements

Financial support by Lahijan Branch, Islamic Azad University Grant No. 17.20.5.3517 is gratefully acknowledged. The authors thank to C. Bambi for valuable suggestions. Also, the authors would like to thank the referees for useful comments.

References

[1] See for instance S.W. Hawking, G. Ellis, The Large Scale Structure of Space-Time, Cambridge University Press, Cambridge, 1973.
[2] See for a review, S. Ansoldi, arXiv:0802.0330.
[3] J.M. Bardeen, in: Conference Proceedings of GR5, Tbilisi, USSR, 1968, p. 174.
[4] S.A. Hayward, Phys. Rev. Lett. 96 (2006) 031103, arXiv:gr-qc/0506126.
[5] J.C.S. Neves, A. Saa, Phys. Lett. B 734 (2014) 44, arXiv:1402.2694.
[6] K. Lin, J. Li, S. Yang, Int. J. Theor. Phys. 52 (2013) 3771.
[7] G. Abbas, U. Sabiullah, Astrophys. Space Sci. 352 (2014) 769, arXiv:1406.0840.
[8] U. Debnath, Eur. Phys. J. C 75 (2015) 129, arXiv:1503.01645.
[9] B. Pourhassan, M. Faizal, Ujjal Debnath, Eur. Phys. J. C 76 (2016) 145, arXiv:1603.01457.
[10] M. Azreg-Aïnou, Phys. Rev. D 90 (2014) 064041, arXiv:1405.2569.

[11] V.P. Frolov, J. High Energy Phys. 05 (2014) 49, arXiv:1402.5446.
[12] E.O. Kahya, M. Khurshudyan, B. Pourhassan, R. Myrzakulov, A. Pasqua, Eur. Phys. J. C 75 (2015) 43, arXiv:1402.2592.
[13] T.D. Lorenzo, C. Pacilioy, C. Rovelli, S. Speziale, Gen. Relativ. Gravit. 47 (2015) 41, arXiv:1412.6015.
[14] T.D. Lorenzo, A. Giusti, S. Speziale, Gen. Relativ. Gravit. 48 (2016) 31, arXiv:1510.08828.
[15] E. Ayón-Beato, A. García, Phys. Rev. Lett. 80 (1998) 5056, arXiv:gr-qc/9911046.
[16] E. Ayón-Beato, A. García, Phys. Lett. B 464 (1999) 25, arXiv:hep-th/9911174.
[17] E. Ayón-Beato, A. García, Gen. Relativ. Gravit. 31 (1999) 629, arXiv:gr-qc/9911084.
[18] E. Ayón-Beato, A. García, Phys. Lett. B 493 (2000) 149, arXiv:gr-qc/0009077.
[19] M. Born, L. Infeld, Proc. R. Soc. Lond. A 144 (1934) 425.
[20] E.S. Fradkin, A.A. Tseytlin, Phys. Lett. B 163 (1985) 123.
[21] A.A. Tseytlin, Nucl. Phys. B 276 (1986) 391.
[22] N. Seiberg, E. Witten, J. High Energy Phys. 9909 (1999) 032, arXiv:hep-th/9908142.
[23] E.L.B. Junior, M.E. Rodrigues, M.J.S. Houndjo, J. Cosmol. Astropart. Phys. 10 (2015) 060, arXiv:1503.07857.
[24] Z-Y. Fan, Eur. Phys. J. C 77 (2017) 266, arXiv:1609.04489.
[25] Z-Y. Fan, X. Wang, Phys. Rev. D 94 (2016) 124027, arXiv:1610.02636.
[26] B. Toshmatov, Z. Stuchlík, B. Ahmedov, Phys. Rev. D 95 (2017) 084037, arXiv:1704.07300.
[27] E. Ayón-Beato, A. García, Gen. Relativ. Gravit. 37 (2005) 635, arXiv:hep-th/0403229.
[28] K.A. Bronnikov, J.C. Fabris, Phys. Rev. Lett. 96 (2006) 251101, arXiv:gr-qc/0511109.
[29] W. Berej, J. Matyjasek, D. Tryniecki, M. Woronowicz, Gen. Relativ. Gravit. 38 (2006) 885, arXiv:hep-th/0606185.
[30] M. Azreg-Aïnou, Phys. Lett. B 730 (2014) 95, arXiv:1401.0787.
[31] L. Balart, E.C. Vagenas, Phys. Lett. B 730 (2014) 14, arXiv:1401.2136.
[32] I. Radinschi, F. Rahaman, T. Grammenos, A. Spanou, S. Islam, Adv. Math. Phys. 2015 (2015) 530281, arXiv:1404.6410.
[33] I. Dymnikova, E. Galaktionov, Class. Quantum Gravity 32 (2015) 165015, arXiv:1510.01353.
[34] E. Chaverra, J.C. Degollado, C. Moreno, O. Sarbach, Phys. Rev. D 93 (2016) 123013, arXiv:1605.04003.
[35] P. Nicolini, A. Smailagic, E. Spallucci, Phys. Lett. B 632 (2006) 547, arXiv:gr-qc/0510112.
[36] S. Ansoldi, P. Nicolini, A. Smailagic, E. Spallucci, Phys. Lett. B 645 (2007) 261, arXiv:gr-qc/0612035.
[37] K. Nozari, S.H. Mehdipour, Class. Quantum Gravity 25 (2008) 175015, arXiv:0801.4074.
[38] See for a review P. Nicolini, Int. J. Mod. Phys. A 24 (2009) 1229, arXiv:0807.1939.
[39] S.H. Mehdipour, Phys. Rev. D 81 (2010) 124049, arXiv:1006.5215.
[40] P. Chen, Y.C. Ong, D.H. Yeom, Phys. Rep. 603 (2015) 1, arXiv:1412.8366.
[41] C. Bambi, Mod. Phys. Lett. A 26 (2011) 2453, arXiv:1109.4256.
[42] C. Bambi, Phys. Lett. B 730 (2014) 59, arXiv:1401.4640.
[43] U. Debnath, Eur. Phys. J. C 75 (2015) 129, arXiv:1503.01645.
[44] C. Bambi, Z. Cao, L. Modesto, Phys. Rev. D 95 (2017) 064006, arXiv:1701.00226.
[45] B.P. Abbott, et al., LIGO Scientific Collaboration Virgo Collaboration, Phys. Rev. Lett. 116 (2016) 061102, arXiv:1602.03837.
[46] B.P. Abbott, et al., LIGO Scientific Collaboration Virgo Collaboration, Phys. Rev. Lett. 116 (2016) 241102, arXiv:1602.03840.
[47] B.P. Abbott, et al., LIGO Scientific Collaboration Virgo Collaboration, Phys. Rev. Lett. 116 (2016) 131102, arXiv:1602.03847.
[48] B.P. Abbott, et al., LIGO Scientific Collaboration Virgo Collaboration, Phys. Rev. Lett. 116 (2016) 241103, arXiv:1606.04855.
[49] B. Gwak, arXiv:1703.10154.
[50] E.F. Eiroa, C.M. Sendra, Class. Quantum Gravity 28 (2011) 085008, arXiv:1011.2455.
[51] J. Schee, Z. Stuchlík, J. Cosmol. Astropart. Phys. 06 (2015) 048, arXiv:1501.00835.
[52] A. Abdujabbarov, M. Amir, B. Ahmedov, S.G. Ghosh, Phys. Rev. D 93 (2016) 104004, arXiv:1604.03809.
[53] S-S. Zhao, Y. Xie, arXiv:1704.02434.
[54] E.T. Newman, A.I. Janis, J. Math. Phys. 6 (1965) 915.
[55] C. Bambi, L. Modesto, Phys. Lett. B 721 (2013) 329, arXiv:1302.6075.
[56] Y.S. Myung, Y-W. Kim, Y.J. Park, Phys. Lett. B 656 (2007) 221, arXiv:gr-qc/0702145.
[57] Y.S. Myung, Y-W. Kim, Y-J. Park, Gen. Relativ. Gravit. 41 (2009) 1051, arXiv:0708.3145.
[58] C. Moreno, O. Sarbach, Phys. Rev. D 67 (2003) 024028, arXiv:gr-qc/0208090.
[59] N. Breton, Phys. Rev. D 72 (2005) 044015, arXiv:hep-th/0502217.
[60] B. Koch, M. Bleicher, S. Hossenfelder, J. High Energy Phys. 0510 (2005) 053, arXiv:hep-ph/0507138.

[61] J.L. Hewett, B. Lillie, T.G. Rizzo, Phys. Rev. Lett. 95 (2005) 261603, arXiv:hep-ph/0503178.
[62] G.L. Alberghi, R. Casadio, A. Tronconi, J. Phys. G 34 (2007) 767, arXiv:hep-ph/0611009.
[63] L. Modesto, in: Proceedings of the XVII SIGRAV Conference, Turin, September 4–7, 2006, arXiv:hep-th/0701239.
[64] G. Amelino-Camelia, J. Ellis, N.E. Mavromatos, D.V. Nanopoulos, Int. J. Mod. Phys. A 12 (1997) 607, arXiv:hep-th/9605211.
[65] A.F. Ali, Phys. Rev. D 89 (2014) 104040, arXiv:1402.5320.
[66] A.F. Ali, M. Faizal, M.M. Khalil, Phys. Lett. B 743 (2015) 295, arXiv:1410.4765.
[67] V.P. Frolov, Phys. Rev. D 94 (2016) 104056, arXiv:1609.01758.
[68] I. Antoniadis, Phys. Lett. B 246 (1990) 377.
[69] J.D. Lykken, Phys. Rev. D 54 (1996) 3693, arXiv:hep-th/9603133.
[70] E. Witten, Nucl. Phys. B 471 (1996) 135, arXiv:hep-th/9602070.
[71] N. Arkani-Hamed, S. Dimopoulos, G.R. Dvali, Phys. Lett. B 429 (1998) 263, arXiv:hep-ph/9803315.
[72] L. Randall, R. Sundrum, Phys. Rev. Lett. 83 (1999) 3370, arXiv:hep-ph/9905221.
[73] I. Hinchliffe, N. Kersting, Y.L. Ma, Int. J. Mod. Phys. A 19 (2004) 179, arXiv:hep-ph/0205040.
[74] J.M. Conroy, H.J. Kwee, V. Nazaryan, Phys. Rev. D 68 (2003) 054004, arXiv:hep-ph/0305225.
[75] P. Schupp, J. Trampetic, J. Wess, G. Raffelt, Eur. Phys. J. C 36 (2004) 405, arXiv:hep-ph/0212292.
[76] K. Nozari, S.H. Mehdipour, J. High Energy Phys. 03 (2009) 061, arXiv:0902.1945.
[77] S.P. Drake, P. Szekeres, Gen. Relativ. Gravit. 32 (2000) 445, arXiv:gr-qc/9807001.
[78] L. Modesto, P. Nicolini, Phys. Rev. D 82 (2010) 104035, arXiv:1005.5605.
[79] I. Arraut, D. Batic, M. Nowakowski, J. Math. Phys. 51 (2010) 022503, arXiv:1001.2226.
[80] A.F. Ali, M. Faizal, M.M. Khalil, Nucl. Phys. B 894 (2015) 341, arXiv:1410.5706.
[81] P. Nicolini, J. Phys. A 38 (2005) L631, arXiv:hep-th/0507266.
[82] S.H. Mehdipour, M.H. Ahmadi, Astrophys. Space Sci. 361 (2016) 314, arXiv:1604.06272.